ЖУРНАЛ СТРУКТУРНОЙ ХИМИИ

2015. Том 56, № 1 *Январь – февраль* *С. 99 – 108*

UDC 548.73:547.13:546.56

A NEW PENTACOORDINATE POLYMERIC COPPER(II) COMPLEX WITH 2-AMINO-2-METHYL-1,3-PROPANDIOL: STRUCTURAL INVESTIGATIONS USING XRD AND DFT

G. Abbas[1], A. Hassan[2], A. Irfan[3], M. Mir[1], Mariya-al-Rashida[4], G. Wu[5]

[1]*Interdisciplinary Research Centre in Biomedical Materials, COMSATS Institute of Information Technology Lahore 54700, Pakistan*
E-mail: abbas191@gmail.com
[2]*Institute of Chemistry, University of the Punjab, Lahore, Pakistan*
[3]*Department of Chemistry, Faculty of Science, King Khalid University, Abha 61413, P.O. Box 9004, Saudi Arabia*
[4]*Department of Chemistry, Forman Christian College (A Chartered University), Ferozepur Road-54600, Lahore, Pakistan*
[5]*State Key Laboratory of Inorganic Synthesis & Preparative Chemistry, Jilin University, 2699 Qianjin Street, Changchun 130012, P. R. China*

Received June, 24, 2013

A novel mononuclear copper complex [Cu(NH_2mpdH)(NH_2mpd)$_2$Cl] (**1**) is synthesized from 2-amino-2-methyl-1,3-propandiol (ampdH_4). The crystal structure of (**1**) is determined using X-ray diffraction studies. The copper complex crystallizes in the triclinic space group *P*-1(2) with $a = 6.10.48(4)$ Å, $b = 10.0915(7)$ Å, $c = 10.9249(9)$ Å, $\alpha = 95.925(6)°$, $\beta = 101.830(6)°$, $\gamma = 90.637(5)°$, $V = 649.53(95)$ Å^3 and $Z = 2$. The central copper(II) atom in (**1**) is coordinated by three oxygen and two nitrogen atoms possessing a five-coordinate distorted square pyramidal geometry arranged in a one dimensional polymeric chain. The ground state geometry of the mononuclear copper complex is optimized using the DFT/B3LYP/6-31G** (LANL2DZ) level of theory. Intra-molecular charge transfer is investigated based on the frontier molecular orbitals. The distribution pattern of the highest occupied molecular orbital and the lowest unoccupied molecular orbital is studied. Absorption spectra are computed using The time dependent density functional theory (TDDFT). The absorption wavelengths are calculated using different functionals, i.e., BHandHLYP, CAM-B3LYP, and LC-BLYP.

K e y w o r d s: copper complex, frontier molecular orbitals, absorption spectrum, density functional theory, time dependent density functional theory.

INTRODUCTION

Coordination chemistry of copper complexes has attained considerable interest due to their aesthetically pleasing structures. Mononuclear copper complexes have exhibited antimicrobial activity [1], optical activities [2], and luminescence properties [3]. Copper complexes are well studied in terms of their kinetics and thermodynamics [4], thermal [5] and magnetic behaviour [6], their chemistry and reactions in metal organic frameworks [7], and charge transfer reactions [8]. DFT and vibrational studies have been frequently used to investigate the structural parameters [9]. Polyalcholic ligands have been employed to produce transition metal complexes due to their good affinity to metal ions [10]. The synthesis of such complexes is facilitated by chelate-forming molecules which contain alkoxide arms that act as good metal-bridging groups and foster the formation of bridged complexes [11]. Dipodal and tripodal ligands, e.g. N-methyldiethanolamine (mdeaH_2) and triethanolamine (tea) respectively, have been used in our previous studies for the synthesis of various multinuclear metal

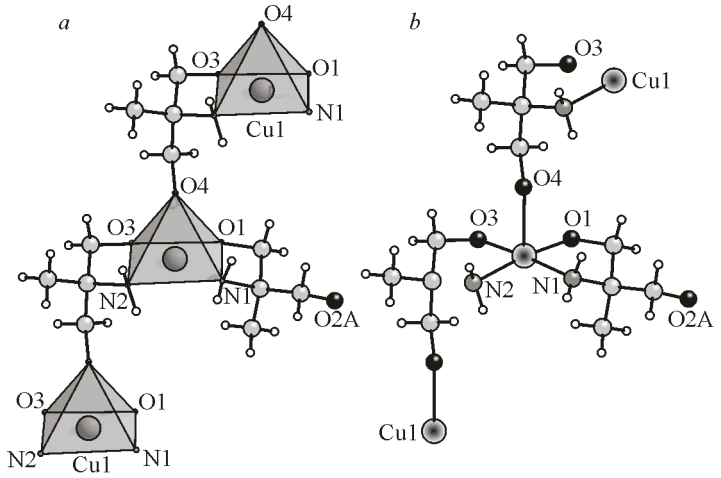

Fig. 1. Molecular structure of the title compound (**1**) presenting a distorted square pyramidal geometry, (*a*) with polyhedral representation (*b*) without polyhedral representation

complexes. The chelating N-methyldiethanolamine ligand in conjugation with pivalic acid yielded dinuclear lanthanide complexes [12], tetranuclear lanthanide aggregates [13], and heteronuclear decanuclear Fe—Dy complexes [14]. We also reported the first octanuclear Fe—Dy single molecular magnet with the tripodal triethanolamine ligand [15]. Another 2-amino-2-methyl-1,3-propandiol ($ampdH_4$) ligand has been used to synthesize Fe, Mn, and Mn—Ni complexes which exhibited interesting magnetic properties [16]. Recently, we investigated the $ampdH_4$ ligand and reported a tetranuclear lanthanide series [17] and DFT studies on Ni cubane [18].

In continuation of our search for novel metal complexes with interesting properties, we have used $amdH_4$ for further coordination with copper metal ions. Herein, we report the synthesis and DFT studies of a new mononuclear copper complex in a distorted square pyramidal geometry (Fig. 1) of the general formula $[Cu(NH_2mpdH)(NH_2mpd)_2Cl]$. The synthesis of mononuclear copper complex is represented in Scheme 1.

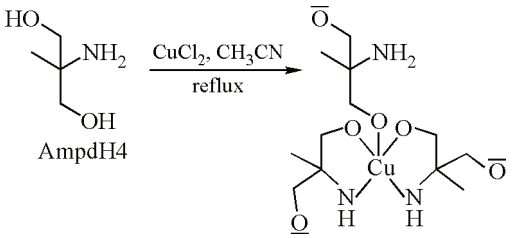

Scheme 1. Schematic representation of the synthesis of $[Cu(NH_2mpdH)(NH_2mpd)_2Cl]$ (**1**)

EXPERIMENTAL

Materials and physical measurement. All chemicals and solvents used were obtained from commercial sources and were used as received without further purification. All reactions were carried out under aerobic conditions. The elemental analyses (C, H, N) were carried out on an Elementar Vario EL analyzer. FTIR spectra were measured on a Perkin-Elmer Spectrum One spectrometer; samples prepared as KBr discs. Single crystal X-ray diffraction patterns were measured at room temperature using a Stoe STADI-P diffractometer with CuK_α radiation at the University of Cyprus, Cyprus.

Synthesis of $[Cu(NH_2mpdH)(NH_2mpd)_2Cl]$ (1). A solution of 2-amino-2-methyl-1,3-propandiol (0.078 g, 0.75 mmol) in MeCN (15 ml) was added dropwise over 20 min to a stirred solution of $CuCl_2 \cdot 2H_2O$ (0.042 g, 0.25 mmol) in MeCN (15 ml). The resulting mixture was refluxed for 2 h, fil-

Table 1

Crystal and refinement data for **1**

Molecular formula	$C_8H_{19}CuN_2O_{4.07}$, Cl
Molecular mass	307.42
Crystal system	Triclinic
Space group	*P*-1
Unit cell parameters *a*, *b*, *c*, Å	6.0562(3), 10.0901(7), 10.9275(8)
α, β, γ, deg.	95.946(6), 101.828(5), 90.649(5)
V, Å^3	649.70(7)
ρ_{calc}, g/cm^3	1.571
T, K	293
Radiation; λ, Å[b]	MoK_α; 0.71073
Color	Blue
Crystal shape	Needle
Reflection measured	2275
$\theta_{min, max}$, deg.	2.94, 25.0
Independent reflections	5881
Parameters refined	172
Final *R* factor [$I > 2\sigma(I)$][c,d]	$R1 = 0.0414$, $wR2 = 0.0970$
R factor (all data)[c,d]	$R1 = 0.0551$, $wR2 = 0.1044$
GOOF	1.011
Residual electron density (min / max), e/Å^3	–0.433 / 0.726

[a] Including solvent molecules.
[b] Graphite monochromator.
[c] $R1 = \sum(||F_0| - |F_c||)/\sum|F_0|$.
[d] $wR2 = [\sum[w(F_0^2 - F_c^2)^2]/\sum[wF_0^2)^2]]^{1/2}$ where $w = 1/[\sigma^2(F_0^2) + (mp)^2 + np]$, $p = [\max(F_0^2, 0) + 2F_c^2]/3$, and *m* and *n* are constants.

tered, and allowed to stand undisturbed in a sealed vial. Dark blue needles of (**1**) suitable for X-ray crystallography were obtained after 3 days. The crystals of (**1**) were maintained in a mother liquor for X-ray crystallography. Yield: ~46 %. *Anal. Calc.* for C, H, N. *Found*: C 31.214; H 6.197; N 9.110 %. *Anal. Calc.* for: C 31.260; H 6.230; N 9.114 %. IR (KBr): ν (cm^{-1}) = 3223 (m), 3124 (s), 2961 (w), 2956 (w), 2629 (w), 1586 (s), 1453 (m), 1399 (s) 1358 (w), 1151 (m), 1361 (m), 1034 (w), 935 (m), 906 (m), 865 (s),774 (m) 724 (w).

X-ray crystallographic data of complex (1). Data were collected on an Oxford-Diffraction diffractometer, equipped with a CCD area detector and a graphite monochromator utilizing MoK_α radiation (λ = 0.71073 Å). A suitable crystal was attached to glass fibers using paratone-N oil and transferred to a goniostat where it was cooled for data collection. Unit cell dimensions were determined and refined using 3823 ($2.94 \le \theta \le 28.80°$) reflections. Empirical absorption correction (multi-scan based on symmetry-related measurements) was applied using the CrysAlis RED software [19]. The structure was solved by direct methods using SIR92 [20] and refined on F^2 using full-matrix least squares using SHELXL97 [21]. Programs used: CrysAlis CCD [18] for data collection, CrysAlis RED [19] for cell refinement and data reduction, and DIAMOND [22] for molecular graphics. The non—H atoms were treated anisotropically, whereas the hydrogen atoms were placed in calculated, ideal positions and refined as riding on their respective carbon atoms. Unit cell data and structure refinement details are listed in Table 1. Full details can be found in the CIF files deposited with the Cambridge

Crystallographic Data Center, CCDC No. 936419. The structure contains severely disordered lattice solvent molecules (CH_3CN, MeOH, H_2O) that could not be modeled properly; thus the SQUEEZE program, a part of the PLATON package of crystallographic software, was used to calculate the solvent disorder area and remove its contribution from the intensity data [23].

COMPUTATIONAL METHODS

The LanL2DZ basis set is used for post-3rd row atoms which used effective core potentials. Recently, the ground state geometries of Cu complexes containing the tripodal tetramine ligand have been computed at two different levels of theories, i.e., B3LYP/LanL2DZ and B3LYP/Gen (LanL2DZ was used for Cu and the 6-31G** basis set for all other atoms). Both levels of theories reproduced the experimental geometrical parameters with a deviation of 0.1 Å in bond distances and 9.5° in bond angles [24]. Previously, DFT has been applied for systems containing transition metals [25]. They concluded that the approaches integrating effective core potentials are efficient in reducing computational expense. In another study, they showed that LANL2DZ was worth attention for transition metals and all-electron basis sets for all other non-transition-metal atoms [26].

The ground state geometry of (**1**) has been optimized using DFT at the B3LYP/6-31** level of theory [27—33]. The LANL2DZ basis set [34—38] was used for the Cu atom, which agrees well with the experimental data and has been found to be reliable for metal containing compounds. Electronic absorption spectra were computed using TD—DFT. The effect of different functionals i.e., correlation functionals B3LYP [39,40] BH, and HLYP [41], hybrid functionals CAM-B3LYP [42], and long-range corrected functionals LC-BLYP [43] on the absorption wavelengths was calculated. The absorption wavelengths computed by different functionals have been compared and discussed. The DOS and UV-Visible Spectra were convoluted using GaussSum 2.1 and Chemcraft softwares, respectively [32, 33, 44]. All the calculations were performed with the Gaussian 09 software [45].

RESULTS AND DISCUSSION

The structure of (**1**) was determined by single crystal X-ray diffraction. The compound was crystallized in the triclinic space group *P*-1(2) with $Z = 2$. Selected bond lengths are given in Table 1. The crystal structure of **1** reveals that the central Cu atom is chelated by two 2-amino-2-methyl-1,3-propandiol ligands, in which both nitrogen atoms are still protonated with Cu(1)—N(1) and Cu(1)—N(2) bonds of 2.006(3) Å and 2.010(3) Å respectively. The oxygen atoms are deprotonated with Cu(1)—O(3) and Cu(1)—O(4) bonds of 1.942(2) Å and 2.387(2) Å respectively. The structure indicates a bis-chelate complex containing two ampd ligands, where (O2A) one ligand remains in the protonated form. The third ampd ligand has monodentate ligation through deprotonated (O4). The central copper(II) atom is penta-coordinated in a distorted square pyramidal CuN_2O_3 geometry. Chloride ions have Cl---H interactions, and Cl---H and Cl---Cl bond distances are 2.8102(8) Å and 5.3228(13) Å respectively. One dimensional chain of mononuclear copper is given in Fig. 2. The chloride ions connect five units through Cl---NH and Cl---HC to make one dimensional polymer chains as shown in Fig. 3.

Geometries and electronic properties. The geometrical parameters, bond lengths, and bond angles have been tabulated in Table 2 (atom numbering scheme is given in Fig. 4). Our computed bond angles are in excellent agreement with the experimental data. Moreover, the computed bond distances are also in reasonable agreement with experimental evidences. The computed bond lengths are somewhat smaller than the experimental values because the computed geometrical bond distances belong to isolated molecules in a gaseous phase while the experimental results belong to molecules in the solid state.

Fig. 5 illustrates the calculated pattern of the highest occupied molecular orbitals (HOMO and HOMO-1) and the lowest unoccupied molecular orbitals (LUMO and LUMO+1). The HOMO-1 is distributed on the left and right ligands which are attached to the central metal, and also Cu and N_{42} atoms make contributions to the formation of HOMO-1. The HOMO is distributed on the left ligand, while Cu, O_3 and N_{42} atoms make also contributions to the formation of HOMO. The acetyl group also takes part in the formation of HOMO. The LUMO is of the anti-bonding character with π^* distributed

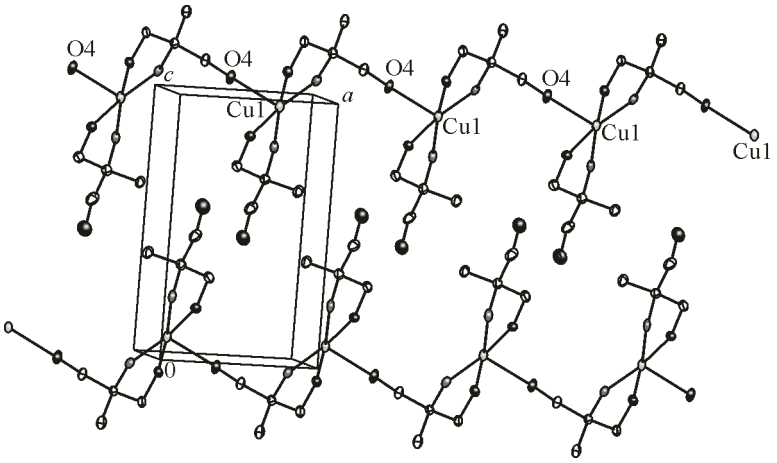

Fig. 2. Packing diagram of one dimensional polymeric chains of (**1**).
H atoms have been removed for the sake of clarity

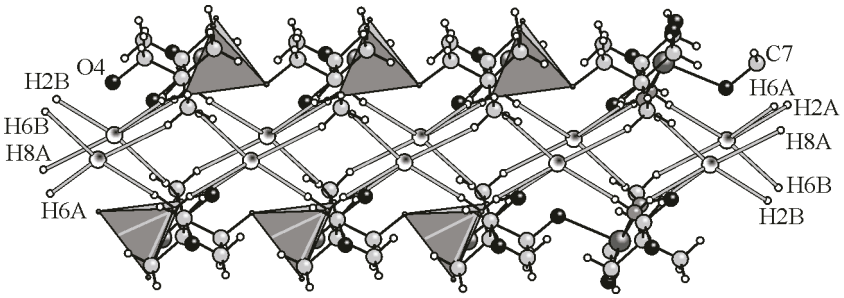

Fig. 3. One dimensional chain connected through Cl atoms (green) having Cl---HN and Cl---HC interactions

T a b l e 2

The bond lengths (Å) *and bond angles* (deg.) *of* (**1**) *in the ground state at the* B3LYP/6-31G** (LANL2DZ) *level of theory*

Bond length, Å			Bond angles, deg.		
	Opt	exp		Opt	Exp
Cu1—O3	1.880	1.947	N5—Cu1—O2	172.78	173.34
Cu1—O2	1.817	1.941	O3—Cu1—O2	93.45	93.36
Cu1—N5	1.911	2.006	N5—Cu1—O2	86.57	84.17
Cu1—N6	1.985	2.011			

on the left and right ligands while LUMO+1 is localized on the top propyl ligand. From the HOMO and LUMO distribution pattern (see the bottom view for clarity), the intramolecular charge transfer has been observed. The HOMO-LUMO energy gap of this compound was calculated at the B3LYP/6-31G* (LANL2DZ) level of theory.

In diverse physical systems density of states (DOS) plays a very important role. In Fig. 5, HOMO and LUMO has been shown by green and blue lines respectively. The HOMO and LUMO energies have been observed to be –6.29 eV and –3.58 eV respectively. The region between the green and blue lines demonstrates the HOMO—LUMO energy gap of 2.71 eV. The energies of HOMO-1 and HOMO-2 are –6.51 and –6.68 eV respectively. The energies of different adjacent occupied molecular orbitals have a very small difference, e.g., energy differences between HOMO-1 and HOMO-2,

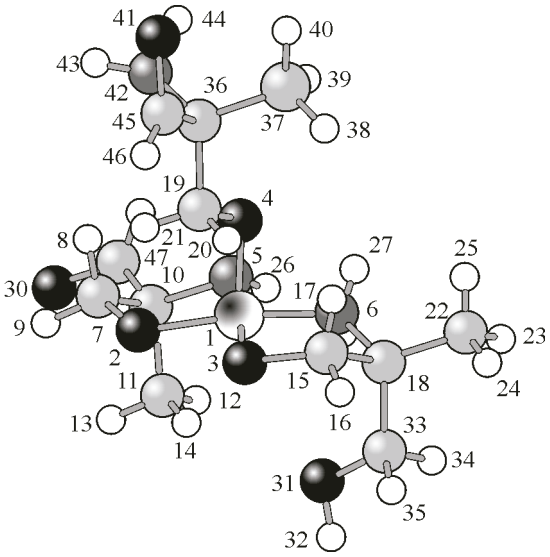

Fig. 4. Molecular structure of the mononuclear copper complex

HOMO-2 and HOMO-3 etc. The energy of LUMO+1 (–1.18 eV) is higher than energy of LUMO (–3.58 eV). The energy of LUMO+2 has been observed to be –0.58 eV while the energies of higher unoccupied molecular orbitals (LUMO+3, LUMO+4, LUMO+5 etc.) are positive (Fig. 5). It would be easy to transfer the electron from HOMO to LUMO and difficult to excite it from HOMO to LUMO+1 or higher unoccupied molecular orbitals.

Absorption spectra. The calculated absorption wavelengths have been illustrated in Fig. 6. The computed absorption wavelengths at the TD-CaM-B3LYP/6-31G** level of theory has been observed in the range 329—571 nm. The first peak has been seen at 329 nm; the second peak at 349 nm. The maximum absorption wavelength, which is the third peak,

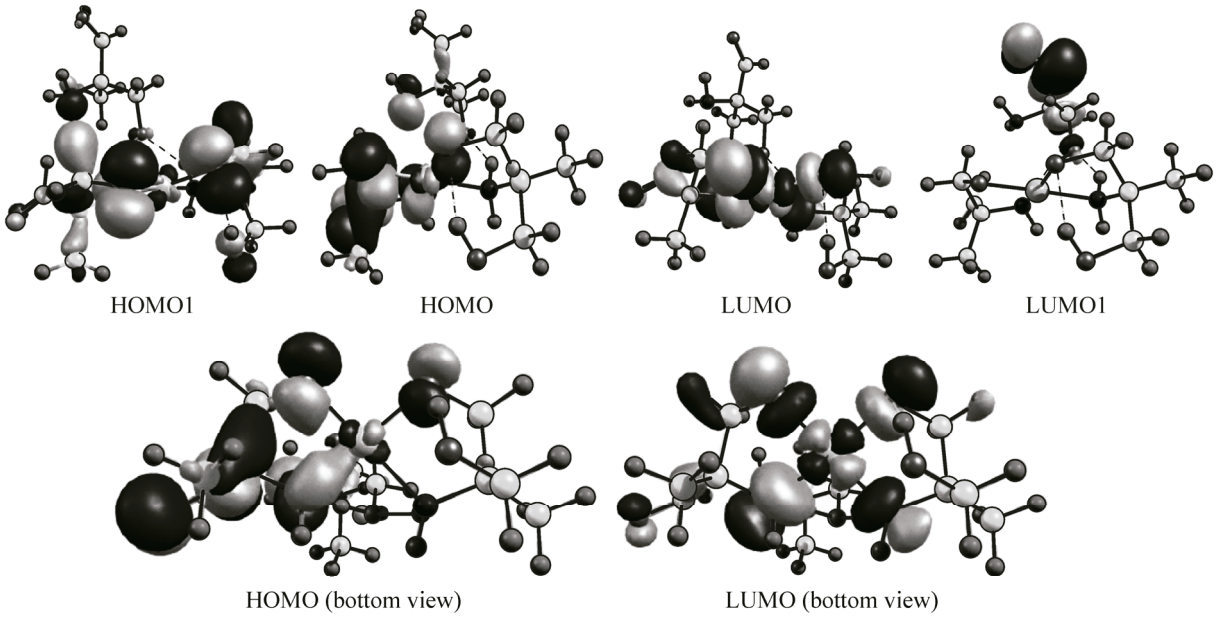

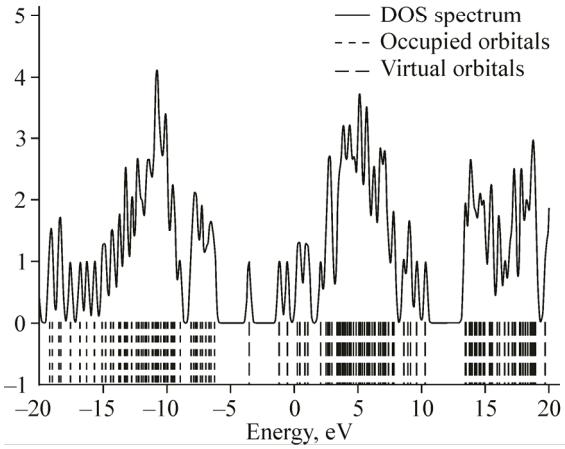

Fig. 5. Distribution patterns of the frontier molecular orbitals (top) and density of state (bottom) at the B3LYP/6-31G** (LANL2DZ) level of theory

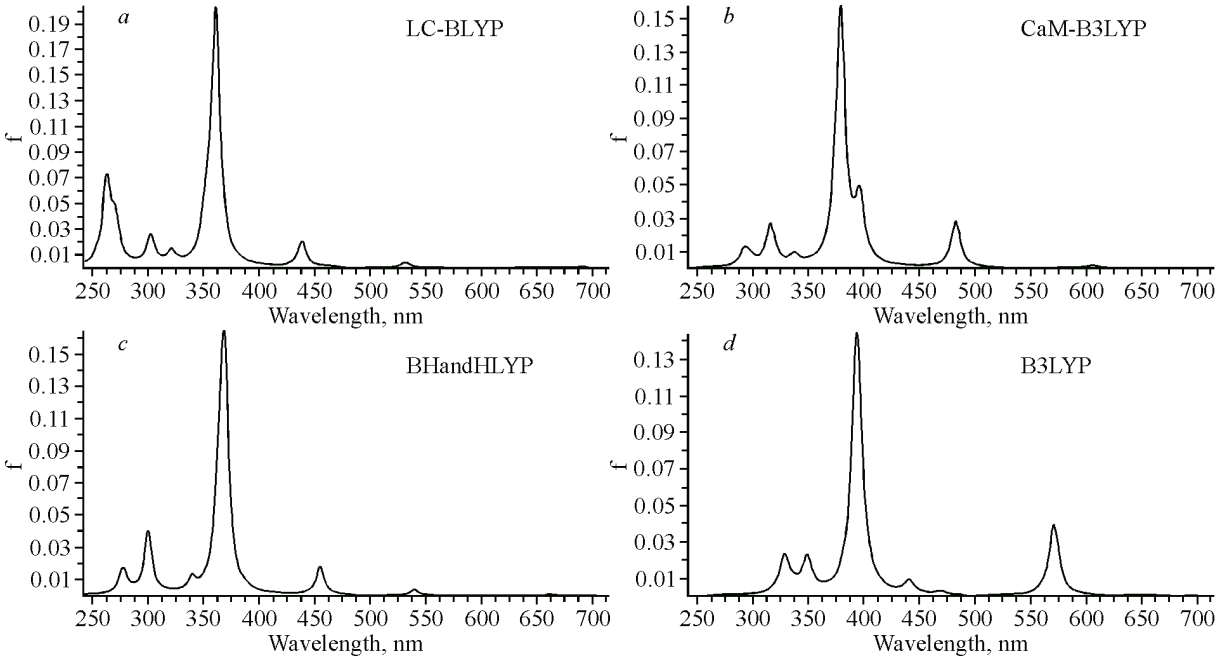

Fig. 6. Computed absorption wavelengths in nm (X axis) and oscillator strengths (Y axis) at (*a*) LC-BLYP; (*b*) CaM-B3LYP; (*c*) BHandHLYP and (*d*) B3LYP

was observed at 394 nm. The fourth, fifth, and sixth peaks were found at 441 nm, 468 nm, and 571 nm respectively. The calculated absorption wavelengths at the TD-BHandHLYP/6-31G** level of theory has been observed in the range 277—539 nm. The first, second, and third peaks were observed at 277 nm, 300 nm, and 339 nm respectively. The maximum absorption wavelength, which is the fourth peak, was observed at 368 nm. The fifth and sixth peaks can be seen at 454 nm and 539 nm respectively. At the TD-CaM-B3LYP/6-31G** level of theory the absorption wavelengths have been observed in the range 292—605 nm. The first peak has been seen at 291 nm, the second peak at 315 nm, and the third peak at 336 nm. The maximum absorption wavelength, which is the fourth peak, was observed at 378 nm. One shoulder peak is at 395 nm. The fifth and sixth peaks were found at 482 nm and 605 nm respectively. At the TD-LC-BLYP/6-31G** level of theory the absorption wavelengths have been observed in the range 263—531 nm. The first, second, and third peaks were observed at 263 nm, 302 nm, and 321 nm respectively. The maximum absorption wavelength, which is the fourth peak, was observed at 361 nm. The fifth and sixth peaks were found at 438 nm and 531 nm respectively.

The experimental absorption spectrum of the studied complex has been measured in ethanol. The first peak, which is the maximum absorption wavelength, has been observed at 328 nm and the second peak at 620 nm (Fig. 7). At the TD-CAM-B3LYP/6-31G** level of theory, the maximum absorption wavelength is overestimated by 66 nm and the last peak is underestimated by 49 nm. At the TD-BHandHLYP/6-31G** level of theory the maximum absorption wavelength and the last peak are overestimated and underestimated, i.e., 40 and 81 nm, respectively. The maximum absorption wavelength at the TD-CAM-B3LYP/6-31G** level of theory is overestimated by 50 nm and the last peak is underes-

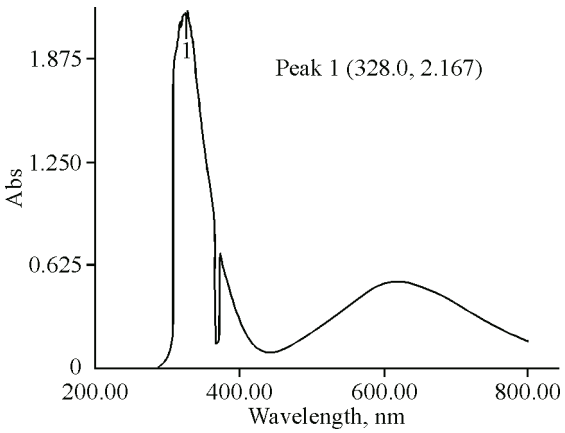

Fig. 7. The absorption wavelength of studied complex measured in ethanol

timated by 15 nm. At the TD-LC-BLYP/6-31G** level of theory the maximum absorption wavelength is overestimated by 33 nm and the last peak is underestimated by 89 nm. Generally, the computed maximum absorption wavelengths at all levels of theories are overestimated while the last absorption peak is underestimated. The absorption wavelengths computed at the TD-CAM-B3LYP/6-31G** level of theory are in better agreement with the experimental data as compared to other level of theories in the present study. Thus the TD-CAM-B3LYP/6-31G** level of theory would be a better choice to compute the absorption wavelengths of the pentacoordinate polymeric copper(II) complex with 2-amino-2-methyl-1,3-propandiol, its derivatives, and similar complexes.

CONCLUSIONS

A new one dimensional copper(II) chain having a distorted square pyramidal geometry has been synthesised using the ampdH_2 ligand. Complete structural investigations were carried out using Fourier Transform Infrared (FT-IR), UV-Visible spectra and single crystal X-ray analysis. DFT and TDDFT studies were carried out for the mononuclear copper complex. The ground state geometry was optimized at the DFT/B3LYP/6-31G** (LANL2DZ) level of theory and the absorption spectra were computed at TD-B3LYP/6-31G** (LANL2DZ). The optimized geometrical parameters are in good agreement with the experimental data. The energies of different adjacent occupied molecular orbitals have a very small difference while the energy difference between the first three unoccupied molecular orbitals is higher. It is expected that the electron transfer from HOMO to LUMO would be favourable while it would be difficult to excite an electron from HOMO to LUMO+1 or higher unoccupied molecular orbitals. The intra-molecular charge transfer has been observed from HOMO to LUMO. The absorption range of the studied compound is from the UV to Vis region. By changing the functional the absorption wavelength varies.

Supplementary data. CCDC 936419 contains the supplementary crystallographic data of complex (**1**) of this article. The data can be obtained free of charge via http://www.ccdc.cam.ac.uk/conts/retrieving.html or from the Cambridge Crystallographic Data Centre, 12 Union Road, Cambridge CB2 IEZ UK; Fax (+44) 1223-336-033; or email: deposit@ccdc.cam.ac.uk Supplementary data associated with this article can be found in the online version.

Acknowledgements. We are grateful to COMSATS Institute of Information Technology Islamabad, Pakistan for the financial support of this research. A. Irfan is thankful to King Khalid University for the support and facilities to carry out the computational research work.

REFERENCES

1. a) *Tsiaggali M.A., Andreadou E.G., Hatz.idimitriou A.G., Pantazaki A.A., Aslanidis P.* // J. Inorgan. Biochem. – 2013. – **121**. – P. 121. b) *Badiger D.S., Hunoor R.S., Patil B.R., Vadavi R.S., Mangannavar C.V., Muchchandi I.S., Patil Y.P., Nethaji M., Gudasi K.B.* // Inorgan. Chim. Acta. – 2012. – **384**. – P. 197. c) *El-Gammal O.A., Abu El-Reash G.M., El-Gamil M.M.* // Spectrochim. Acta Part A: Mol., Biomol. Spectr. – 2012. – **96**. – P. 444. d) *Mohan N. Patel, Hardik N. Joshi, Chintan R. Patel* // Spectrochim. Acta Part A: Mol., Biomol. Spectr. – 2013. – **104**. – P. 48. e) *Sayen S., Carlier A., Tarpin M., Guillon E.* // J. Inorgan. Biochem. – 2013. – **120**. – P. 39.
2. *Kumar A., Mayer-Figge H., Sheldrick W.S., Singh N.* // Eur. J. Inorg. Chem. – 2009. – P. 2720.
3. a) *Hou T., Bian J., Yue X., Yue S., Ma J.* // Inorgan. Chim. Acta. – 2013. – **394**. – P. 15. b) *Volz D., Nieger M., Friedrichs J., Baumann T., Bräse S.* // Langmuir. – 2013. – **29**. – P. 3034. c) *He L.H., Chen J.L., Zhang F., Cao X.F., Tan X.Z., Chen X.X., Rong G., Luo P., Wen H.R.* // Inorg. Chem. Commun. – 2012. – **21**. – P. 125.
4. a) *Ozay H., Baran Y.* // J. Coord. Chem. – 2010. – **63**. – P. 4299. b) *Balaghi S.E., Safaei E., Rafiee M., Kowsari M.H.* // Polyhedron. – 2012. – **47**. – P. 94.
5. *Madarasz J., Bombicz P., Czugler M., Pokol G.* // Polyhedron. – 2000. – **19**. – P. 457.
6. a) *Naiya S., Biswas S., Drew M.G.B., García C.J.G., Ghosh A.* // Inorgan. Chim. Acta. – 2011. – **377**. – P. 26. b) *Zhu X., Wang N., Li B., Zhang H., Luo Y., Pang Y., Tian D.* // Inorgan. Chim. Acta. – 2012. – **383**. – P. 235. c) *Zhao F.H., Che Y.X., Zheng J.M.* // Inorg. Chem. – 2012. – **51**. – P. 4862. d) *Muñoz S., Pons J., Ros J., Bardia M.F., Kilner C.A., Halcrow M.A.* // Inorgan. Chim. Acta. – 2011. – **373**. – P. 211. e) *Li H., Zhang S.G., Xie L.M., Yu L., Shi J.M.* // J. Coord. Chem. – 2011. – **64**. – P. 1456.

7. *Ibrahim A.O., Zhou Y., Jiang F., Chen L., Li X., Xu W., Onawumi O.O.E., Odunola O.A., Hong M.* // Eur. *J. Inorg. Chem*. – 2011. – P. 5000.
8. a) *Kern T., Monkowius U., Zabel M., Knör G.* // Eur. J. Inorg. Chem. – 2010. – P. 4148. b) *Klein A., Butsch K., Neudörfl J.* // Inorg. Chim. Acta. – 2010. – **363**. – P. 3282.
9. a) *Machura B., Switlicka A., Palion J., Kruszynski R.* // Struct. Chem. – 2013. – **24**. – P. 89. b) *Costa A.C. Jr., Ramos J.M., Soto C.A.T., Martin A.A., Raniero L., Ondar G.F., Versiane O., Moraes L.S.* // Spectrochim. Acta Part A: Mol., Biomol. Spectr. – 2013. – **105**. – P. 259. c) *Shen Y.F., Fang C.J., Peng Z.H., Lia D.C., Zhou Y.H.* // Spectrochim. Acta Part A: Mol., Biomol. Spectr. – 2005. – **62**. – P. 132. d) *Sharma R.P., Saini A., Venugopalan P., Jezierska J., Ferretti V.* // Inorg. Chem. Commun. – 2012. – **20**. – P. 209. e) *Pedras B., Oliveira E., Santos H., Rodríguez L., Crehuet R., Avilés T., Capelo J.L., Lodeiro C.* // Inorg. Chim. Acta. – 2009. – **362**. – P. 2627. f) *Diéguez A.R., Viseras M.E.L., Buceta J.E.P., Mota A.J., Colacio E.* // Inorg. Chim. Acta. – 2012. – **385**. – P. 73. g) *Cañellas P., Bauzá A., Raso A.G., Fiol J.J., Deyà P.M., Molins E., Mata I., Frontera A.* // Dalton Trans. – 2012. – **41**. – P. 11161.
10. *Tasiopoulos A.J., Perlepes S.P.* // Dalton Trans. – 2008. – P. 5537.
11. a) *Nesterov D.S., Kokozay V.N., Skelton B.W.* // Eur. J. Inorg. Chem. – 2009. – P. 5469. b) *Sun W.W., Cheng Q., Zhou H., Pan Z.* // J. Coord. Chem. – 2013. – **66**. – P. 56. c) *Liu J., Ma C., Chen H., Hu M., Wen H., Cui H., Song X., Chen C.* // Dalton Trans. – 2013. – **42**. – P. 2423. d) *Barman T.R., Sutradhar M., Drew M.G.B., Rentschler E.* // Polyhedron. – 2013. – **51**. – P. 192.
12. *Abbas G., Lan Y., Kostakis G., Anson C.E., Powell A.K.* // Inorg. Chim. Acta. – 2008. – **361**. – P. 3494.
13. *Abbas G., Lan Y., Kostakis G.E., Wernsdorfer W., Anson C.E., Powell A.K.* // Inorg. Chem. – 2010. – **49**. – P. 8067.
14. *Abbas G., Lan Y., Mereacre V., Wernsdorfer W., Clérac R., Buth G., Sougrati M.T., Grandjean F., Long G.J., Anson C.E., Powell A.K.* // Inorg. Chem. – 2009. – **48**. – P. 9345.
15. *Schray D., Abbas G., Lan Y., Mereacre V., Kostakis G., Anson C.E., Powell A.K.* // Angew. Chem. – 2010. – **49**. – P. 5185.
16. a) *Kizas C.M., Manos M.J., Nastopoulos V., Boudalis A.K., Sanakis Y., Tasiopoulos A.J.* // Dalton Trans. – 2012. – **41**. – P. 1544. b) *Papatriantafyllopoulou C., Kizas C.M., Manos M.J., Boudalis A., Sanakis Y., Tasiopoulos A.J.* // Polyhedron. – 2013. in press, doi number:0.1016/j.poly.2013.04.035. c) *Charalambous M., Moushi E.E., Papatriantafyllopoulou C., Wernsdorfer W., Nastopoulos V., Christou G., Tasiopoulos A.J.* // Chem. Commun. – 2012. – **48**. – P. 5410. d) *Moushi E.E., Lampropoulos C., Wernsdorfer W., Nastopoulos V., Christou G., Tasiopoulos A.J.* // J. Amer. Chem. Soc. – 2010. – **132**. – P. 16146. e) *Moushi E.E., Stamatatos T.C., Wernsdorfer W., Nastopoulos V., Christou G., Tasiopoulos A.J.* // Inorg. Chem. – 2009. – **48**. – P. 5049.
17. *Abbas G., Kostakis G.E., Lan Y., Powell A.K.* // Polyhedron. – 2012. – **45**. – P. 1.
18. *Abbas G., Rashida M., Irfan A.* // J. Struct. Chem. – 2013. – **55**, N 1. – P. 36 – 42.
19. ″A multipurpose crystallographic tool″, Utrecht University, The Oxford Diffraction 2009. CrysAlis CCD, CrysAlis RED, version p171.33.34d, Oxford Diffraction Ltd, Abingdon, Oxford, England.
20. *Altomare A., Cascarano G., Giacovazzo C., Guagliardi A., Burla M.C., Polidori G., Camalli M.* // SIR92 J. Appl. Crystallogr. – 1994. – **27**. – P. 435.
21. *Sheldrick G.M.* SHELXL97, University of Göttingen, Germany.
22. *Brandenburg K.* DIAMOND. Crystal Impact GbR, Bonn, Germany, 1999.
23. a) *Spek A.L.* PLATON. Netherlands, 2003. b) *van der Sluis P., Spek A.L.* // SQUEEZE: Acta Cryst. Sect. A. – 1990. – **46**. – P. 194.
24. *Karakas D., Sayin K.* // Indian. J. Chem. – 2013. – **52A**. – P. 480.
25. *Riley K.E., Merz K.M. Jr.* // J. Phys. Chem. – 2007. – **111**. – P. 6044.
26. *Yang Y., Weaver M.N., Merz K.M. Jr.* // J. Phys. Chem. A. – 2009. – **113**. – P. 9843.
27. a) *Irfan A., Nadeem M., Athar M., Kanwal F., Zhang J.* // Comp. Theo. Chem. – 2011. – **968**. – P. 8. b) *Irfan A., Al-Sehemi A.G., Muhammad S., Zhang J.* // Aust. J. Chem. – 2011. – **64**. – P. 1587. c) *Al-Sehemi A.G., Irfan A., Asiri A.M.* // Theor. Chem. Acc. – 2012. – **131**. – P. 1199. d) *Al-Sehemi A.G., Al-Melfi M.A.M., Irfan A.* // Struct. Chem. – 2013. – **24**. – P. 499. e) *Irfan A., Al-Sehemi A.G., Kalam A.* // J. Mol. Struc. – 2013. http: // dx.doi.org/10.1016/j.molstruc.2013.06.023. f) *Irfan A., Al-Sehemi A.G., Al-Assiri M.S.* // J. Mol. Graphics, Model. – 2013. http: // dx.doi.org/10.1016/j.jmgm.2013.06.003. g) *Irfan A.* // Mater. Chem. Phys. – 2013. http: // dx.doi.org/10.1016/j.matchemphys.2013.07.011.
28. *Irfan A., Al-Sehemi A.G.* // J. Mol. Model. – 2012. – **18**. – P. 4893.
29. *Jin R., Irfan A.* // Comput. Theor. Chem. – 2012. – **986**. – P. 93.
30. *Irfan A., Hina N., Al-Sehemi A.G., Asiri A.M.* // J. Mol. Model. – 2012. – **18**. – P. 4199.
31. *Irfan A., Al-Sehemi A.G., El-Agrody A.M.* // J. Mol. Struct. – 2012. – **1018**. – P. 171.

32. *Irfan A., Ijaz F., Al-Sehemi A.G., Asiri A.M.* // J. Comput. Electron. – 2012. – **11**. – P. 374.
33. *Al-Sehemi A.G., Al-Amri R.S.A., Irfan A.* // Acta Phys. Chim. Sin. – 2013. – **29**. – P. 1.
34. *Irfan A., Zhang J., Chang Y.* // Chem. Phys. Lett. – 2009. – **483**. – P. 143.
35. *Wan L., Zhang Y.X., Qi D.D., Jiang J.H.* // J. Mol. Graphics Model. – 2010. – **28**. – P. 842.
36. *Liu Z.Q., Chen Z.X., Jin B.B., Zhang X.X.* // Vib. Spectrosc. – 2011. – **56**. – P. 210.
37. *Li L., Tang Q., Li H., Yang X., Hu W., Song Y., Shuai Z., Xu W., Liu Y., Zhu D.* // Adv. Mater. – 2007. – **19**. – P. 2613.
38. *Ma R., Guo P., Yang L., Guo L., Zeng Q., Liu G., Zhang X.* // J. Mol. Struct. – 2010. – **942**. – P. 131.
39. *Walsh P.J., Gordon K.C., Officer D.L., Campbell W.M.* // J. Mol. Struct. – 2006. – **759**. – P. 17.
40. *Cleland D.M., Gordon K.C., Officer D.L., Wagner P., Walsh P.J.* // Spectrochim. Acta A: Mol., Biomol. Spectr. – 2009. – **74**. – P. 931.
41. *Becke A.D.* // J. Chem. Phys. – 1993. – **98**. – P. 1372.
42. *Yanai T., Tew D., Handy N.* // Chem. Phys. Lett. – 2004. – **393**. – P. 51.
43. *Iikura H., Tsuneda T., Yanai T., Hirao K.* // J. Chem. Phys. – 2001. – **115**. – P. 3540.
44. *O'Boyle N.M., Tenderholt A.L., Langner K.M.* // J. Comp. Chem. – 2008. – **29**. – P. 839.
45. *Frisch M.J. et al.* Gaussian 09 Revision A.1 Gaussian Inc. Wallingford, CT, 2009.